

Author's Comments to the Chief Editor

We appreciate the chief editor for precise and clear contributions. We hereby state that all comments have been treated accordingly.

The Transient Variation of the Complexes of the Low Latitude Ionosphere within the Equatorial Ionization Anomaly Region of Nigeria.

A. B. Rabi^{1,2}, B. O. Ogunsua¹, I. A. Fuwape¹ and J. A. Laoye³

[1] {Space Physics Laboratory, Department of Physics, Federal University of Technology, Akure, ~~Ondo State~~, Nigeria}

[2]{Centre for Atmospheric Research, National Space Research and Development Agency, Anyigba, ~~Kogi State~~ Nigeria}

[3] {Department of Physics, Olabisi Onabanjo University, Ago-Iwoye, ~~Ogun State~~, Nigeria}

Correspondence to: B. O. Ogunsua (iobogunsua@futa.edu.ng)

Abstract

The quest to find an index for proper characterization and description of the dynamical response of the ionosphere to external influences and its various internal irregularities has led to the study of the day to day variations of the chaoticity and dynamical complexity of the ionosphere. This study was conducted using Global Positioning System (GPS) Total Electron Content (TEC) time series, measured in the year 2011, from 5 GPS receiver stations in Nigeria which lies within the Equatorial Ionization Anomaly region. The nonlinear aspect of the TEC time series were obtained by detrending the data. The detrended TEC time series were subjected to various analyses to obtain the phase space reconstruction and to compute the chaotic quantifiers which are Lyapunov exponents LE, correlation dimension, and Tsallis entropy for the study of dynamical complexity. Considering all the days of the year the daily/transient variations show no definite pattern for each month but day to day values of Lyapunov exponent for the entire year show a wavelike semiannual variation pattern with lower values around March, April, September and October, ~~a change in pattern which demonstrates the self-organized-critical-phenomenon-of the system~~. This can be seen from the correlation dimension with values between 2.7 and 3.2

31 with lower values occurring mostly during storm periods demonstrating a phase transition from
32 higher dimension during the quiet periods to lower dimension during storms for most of the
33 stations. The values of Tsallis entropy show similar variation pattern with that of Lyapunov
34 Exponent, with both quantifiers correlating within the range of 0.79 to 0.82. These results show
35 that both quantifiers can be further used together as indices in the study of the variations of the
36 dynamical complexity of the ionosphere. The presence of chaos and high variations in the
37 dynamical complexity, even at quiet periods in the ionosphere may be due to the internal
38 dynamics and inherent irregularities of the ionosphere which exhibit non-linear properties.
39 However, this inherent dynamics may be complicated by external factors like Geomagnetic
40 storms. This may be the main reason for the drop in the values of Lyapunov exponent and Tsallis
41 entropy during storms. The dynamical behavior of the ionosphere throughout the year as
42 described by these quantifiers, were discussed in this work.

43

44 **1.0 Introduction**

45 The behavior of natural systems like the ionosphere is a function of changes that occur in the
46 underlying dynamics that exists in such system. These underlying dynamics however can be
47 sometimes complex and nonlinear due to superposition of different changes in dynamical
48 variables that constitute it. ~~When the dynamical states of a system changes suddenly due to~~
49 ~~sudden changes in the external factor affecting the system, then such a system is said to be~~
50 ~~deterministic.~~

51 However, there is no totally deterministic system in nature, because all natural systems exhibit a
52 mixture of both **stochastic and** deterministic properties. Although few natural systems have been
53 found to be low dimensional deterministic in the sense of the theory, the concept of low-
54 dimensional chaos has been proven to be fruitful in the understanding of many complex
55 phenomena (Hegger et al., 1999) The degree of determinism or stochasticity in most natural
56 systems is dependent on how much the system can be influenced by external factors, the nature
57 of these external factors among others .The ionosphere like every other natural system possess its
58 intrinsic dynamics and it can also be influenced by other external factors. The typical
59 characteristics of a dynamical system like the ionosphere is expected to naturally show the
60 interplay between determinism and stochasticity simply because of the fact that the ionosphere

61 which has an inherent internal dynamics is also influenced by the influx of stochastic drivers like
62 the solar wind, since it is influenced by external dynamics like every other natural system. This
63 has made pure determinism impossible in the ionosphere, a situation that is common to all
64 natural system and its surrounding.

65 The intensity of the solar wind coming into the ionosphere varies with the solar activity ~~and an~~
66 ~~extreme solar activity~~ and this can ~~lead sometimes result into~~ geomagnetic storms and substorms
67 drive in high intensity plasma wind at enormous speed and it serves as major stochastic driver
68 leading to storm. The solar wind is driven from the sun into the ionospheric system during the
69 quiet and storm and during relatively quiet periods of each month of the year. However other
70 processes which include various factors like local time variations of the neutral winds, ionization
71 processes, production-recombination rates, photoionization processes, plasma diffusion and
72 various electrodynamic processes. (Unnikrishnan, 2010). The mesosphere and the lower
73 thermospheric dynamics as reported by Kazimirovsky and Vergasova (2009) and also the
74 influence of gravity waves as reported by Sindelarova (2009) can also be of great influence on
75 the internal dynamics of the ionosphere.

76 Therefore, it is of great importance to study the chaoticity and dynamical complexity of the
77 ionosphere and its variations in all geophysical conditions. However a good number of
78 investigations have been carried out on concept of chaos in the upper atmosphere before now
79 which includes the study on magnetospheric dynamics and the ionosphere. The study of chaos in
80 magnetospheric index time series such as AE and AL were initially carried out by (Vasiliadis et
81 al., 1990, Shan et al, 1999; Pavlos et al, 1992). These previous efforts made by the
82 aforementioned researchers has led to the development of the concept of investigating and
83 revealing the chaoticity and the complex dynamics of the ionosphere, and as a result, studies on
84 the chaoticity of the ionosphere have been conducted, by some investigators like Bhattacharyya
85 (1990) who studied chaotic behavior of ionospheric diversity fluctuation using amplitude and
86 phase scintillation data, and found the existence of low dimension chaos. Also, Wernik and Yeh
87 (1994) further revealed the chaotic behavior of the ionospheric turbulence using scintillation data
88 and numerical modeling of scintillation at high latitude. They showed that the ionospheric
89 turbulence attractor (if it exists) cannot be reconstructed from amplitude scintillation data and
90 their measured phase scintillation data adequately reproduce the assumed chaotic structure in the

91 ionosphere. Also Kumar et al., (2004) reported the evidence of chaos in the ionosphere by
92 showing the chaotic nature of the underlying dynamics of the fluctuations of TEC power
93 spectrum indicating exponential decay and the calculated positive value of Lyapunov exponent.
94 This is also supported by the results of the comparison of the chaotic characteristics of the time
95 series of variations of TEC with the pseudochaotic characteristic of the colored noise time series.
96 Xuann et al., (2006) studied chaos properties of ionospheric total electron content (TEC) using
97 TEC data from 1996 to 2004, and analyze possibility to predict it by using chaos. They found
98 the presence of chaos in the TEC measured in the study area, as indicated by the positive
99 Lyapunov exponent computed from their data. The correlation dimension was 3.6092 from their
100 estimation. They were also able to show that the TEC time series can be predicted using chaos.

101

102 Also, Unnikrishnan et al (2006a,b) have analyzed the deterministic chaos in mid latitude and
103 Unnikrishnan (2010), Unnikrishnan and Ravindran (2010), analyzed some TEC data from some
104 Indian low latitude stations for quiet period and major storm period and found in Their results the
105 presence of chaos which was indicated by a positive Lyapunov exponent, and they also inferred
106 that storm periods exhibits lower values compared to quiet periods. The dynamical complexity
107 of magnetospheric processes and the ionosphere have been studied by a number of researchers.
108 Balasis et al., (2008) investigated the dynamical complexity of the magnetosphere by using
109 Tsallis entropy as a dynamical complexity measure in D_{st} time series also Balasis et al., (2009)
110 investigated the dynamical complexity in D_{st} further by considering different entropy measures.
111 Coco et al (2011) using the information theory approach studied the dynamical changes of the
112 polar cap potential which is characteristic of the polar region ionosphere by considering three
113 cases (i) steady IMF $B_z > 0$, (ii) steady IMF $B_z < 0$ and (iii) a double rotation from negative to
114 positive and then positive to negative B_z . They observed a neat dynamical topological transition
115 when the IMF B_z turns from negative to positive and vice versa, pointing toward the possible
116 occurrence of an order/disorder phase transition, which is the counterpart of the large scale
117 convection rearrangement and of the increase of the global coherence. Further studies ~~in~~ on the
118 chaotic behavior and nonlinear dynamics of the ionosphere over the low latitude African region
119 is however ~~needed~~ required ~~to~~ for the improvement of our understanding and characterization of
120 ~~the its~~ dynamical behavior. ~~of the ionosphere of low latitude ionosphere especially over Africa~~

121 ~~during quiet and storm for different season of the year some as to be able to characterize~~
122 ~~chaoticity for different season of the year for quiet and storm periods.~~ Recently Ogunsua et al
123 (2014) studied comparatively the chaoticity of the equatorial ionosphere over Nigeria using TEC
124 data, considering five quietest day classification and five most disturbed day classification. They
125 were able to show the presence of chaos as indicated the positive Lyapunov exponents and also
126 were able to show that Tsallis entropy can be used as a viable measure of dynamical complexity
127 in the ionosphere with portions showing lower values of Tsallis entropy indicating lower
128 dynamical complexity, with a good relationship with Lyapunov exponents. They found a phase
129 transition from higher dimension during quiet days to Lower dimension during storm.

130

131 The low latitude region where Nigeria is situated is known as the equatorial anomaly region, ~~this~~
132 ~~region is known for equatorial ionization anomaly, which is due to the fountain effect. where the~~
133 ~~magnetic field B is almost totally parallel to the equator.~~ Off the equator the E region electric
134 field maps ~~map~~ along the magnetic field up to the F-region altitude in the low latitude, this
135 eastward electric field (E) interacts with the magnetic field B at the F region during the day. This
136 results in the electrodynamic lifting of the F-region plasma over the equator, known as EXB
137 drift. The uplifted plasma over the equator moves along the magnetic line in response to gravity,
138 diffusion and pressure gradients and hence, the fountain effect. The fountain effect being
139 controlled by the EXB drift shows the dynamics of the diurnal variation equatorial anomaly
140 (Abdu, 1997; Unnikrishnan 2010). There is a reduction in the F region ionization density at the
141 magnetic equator and also much enhanced ionization density at the two anomaly crests within
142 $\pm 15^\circ$ of the magnetic latitude north and south of the equator (Rama Rao et al., 2006). The
143 equatorial ionization anomaly and other natural processes which includes various ionization
144 processes and recombination; influx of solar wind, photoionization processes and so many other
145 factors that occur due to variations in solar activities, have a great influence on the systems of
146 the ionosphere, due to their effects on internal dynamics of the ionosphere. This portrays the
147 ionosphere as a typical natural system with continuous interaction with its external environment
148 which led to the study of the influence of the sun on the ionosphere (Ogunsua et al., 2014).

149 The ionosphere possesses a significant level of nonlinear variations that requires more
150 investigation which can be studied and characterized using nonlinear approach like the chaoticity

151 and dynamical complexity for the study of its dynamics. The need to study the daily variation in
152 the dynamical complexity of the ionosphere arises from the established knowledge and
153 understanding which shows that the ionosphere is a complex system with so many variations that
154 can arise from various dynamical changes that can be due to various changes in different
155 processes that contribute to the behavior and nature of the ionosphere. Rabiou et al., (2007)
156 affirmed that characterizing the ionosphere is of utmost importance due to the numerous
157 complexities associated with the region. The scale of these numerous complexities interestingly
158 changes at times from one day to another.

159 The concept of chaos as previously applied to ionospheric and magnetospheric studies on quiet
160 and stormy conditions are limited. Most investigations have been based on only quiet and storm
161 conditions for all studies carried out, and none of the previous works involved the use of quiet
162 and disturbed day classification of geophysical conditions until recently by Ogunsua et
163 al.,(2014), where we considered the comparative use of Lyapunov exponent and Tsallis entropy
164 as proxies for the internal dynamics of the ionosphere. This is the main reason for the
165 consideration of day to day variation of these parameters in this work.

166 **2.0 Data and Methodology**

167 The data used for this study is the global positioning system (GPS) total electron content (TEC)
168 data obtained from 5 GPS satellite receiver stations. Table 1 shows the coordinates of the
169 stations. These receivers take the measure of slant TEC within 1m^2 columnar unit of the cross
170 section along the ray path of the satellite and the receiver which is given by

$$171 \text{STEC} = \int_{\text{receiver}}^{\text{Satellite}} Ndl \quad (1)$$

172 The observation of the total number of free electron along the ray path are derived from the
173 frequency $L_1(1572.42 \text{ MHz})$ and $L_2(1227.60 \text{ MHz})$ of Global Positioning System(GPS), that
174 provide the relative ionosphere delay of electromagnetic waves travelling through the medium
175 (Saito et al.,1998). The Slant TEC is projected to vertical TEC using the thin shell model
176 assuming the height of 350m (Klobuchar,1986).

177 $VTEC = STEC \cdot \cos[\arcsin(R_e \cos\theta / R_e + h_{max})]$ (2)

178 Where $R_e = 6378km$ (radius of the earth), $h_{max} = 350km$ (the vertical height assumed from
179 the satellite) and $\theta = \text{elevation angle at ground station}$

180

181 In this study, 5 GPS TEC measuring stations lying within the low latitude region were
182 considered, as shown in table 1. The TEC data obtained for January to December 2011 were
183 considered for this study and the data are given at 1min sampling time. The TEC data were
184 subjected to various analyses which will be discussed in the next section. The day to day
185 variations of the chaotic behavior and dynamical complexity were studied for the entire year.
186 The surrogate data tests for non linearity were also conducted for both the dynamical and
187 geometrical aspects.

188 **3.0 Methods of Data Analysis and Results**

189 **3.1 Time series analysis**

190 Time series can be seen as a numerical account that describes the state of a system, from which it
191 was measured. A given time series, S_n can be defined as a sequence of scalar measurement of a
192 particular quantity taken as series at different portion in time for a given time interval(Δt). The
193 time series describe the physical appearance of an entire system, as seen in Fig 1. However it
194 may not always describe the internal dynamics of that system. A system like the ionosphere
195 possesses a dominant dynamics that can be seen as diurnal so the data should be treated so as to
196 be able to see its internal dynamics. The measured TEC time series were plotted to see the
197 dynamics of the system. A typical plot of TEC usually has a dominant dynamics (see fig 1)
198 which may be seen as the diurnal behavior, however, it can also be seen that there is also a
199 presence of fluctuations (which appear to be nonlinear) in the system as a result of the internal
200 dynamics of the ionosphere and space plasma system, due to different activities in the
201 ionosphere. Therefore there is need to minimize the influence of the diurnal variations since we
202 are more interested in the nonlinear internal dynamics of the system in this study, to do so the
203 TEC time series was detrended by carrying out the following analysis below:

204 Since for the given daily data of 1minute sampling time there are 1440 data points per day. Then
 205 there exists a time series t_i , where $i = 1,2,3 \dots 1440$ represents the observed time series, and
 206 there also exists a set of u_i where $i = 1,2,3 \dots 1440$, such that the diurnal variation reduced time
 207 is given by

$$208 \quad T_i = t_i - u_j \quad (3)$$

209 Where $i = 1,2,3, \dots, j = \text{mod}(i, 1440)$, if $\text{mod}(j, 1440) \neq 0$, and $j = 1440$ if $d(j, 1440) = 0$.
 210 This method will give the detrended time series represented by T_i obtained from the original
 211 TEC data as shown in fig 2. This method is similar to that used by (Unnikrishnan et al., 2006,
 212 Unnikrishnan 2010), the further explanations on the dynamical results can be found in (Kumar et
 213 al., 2004). The detrended time series were subjected to further analyses for the Phase space
 214 reconstruction and also to obtain the values of Lyapunov exponents, correlation dimension,
 215 Tsallis entropy and the implementation of surrogate data test.

216

217 **3.1.1 Phase Space reconstruction and Non Linear Time Series Analysis**

218 The study of chaoticity and dynamical complexity in a dynamical system requires a nonlinear
 219 approach, due to the fact that systems described by these phenomena can be referred to as
 220 nonlinear complex systems. The magnetosphere and the ionosphere are good examples of such
 221 systems. To be able to study such phenomena some nonlinear time series analysis can be carried
 222 out on the time series data describing such a system. The detrended time series of TEC
 223 measurement is subjected to some nonlinear time series data analysis to obtain the mutual
 224 information and false nearest neighbours, embedding dimension and delay coordinates for the
 225 phase space reconstruction, and the evaluation of other chaotic quantifiers namely: Lyapunov
 226 Exponents, Correlation dimension, recurrence analysis and Entropy.

227 The phase space reconstruction helps to reveal the multidirectional aspect of the system. The
 228 phase space reconstruction is based on embedding theorem, such that the phase space is
 229 reconstructed to show the multidimensional nature as follows:

$$230 \quad Y_n = (s_{n-(m-1)\tau}, s_{n-(m-2)\tau}, \dots, s_{n-\tau}, s_n) \quad (4)$$

231 where Y_n are vector in phase space. The proper choice of embedding dimension (m) and delay
232 Time (τ) are essential for phase space reconstruction (Fraser and Swinney,1986; Kennel et
233 al.,1992) .

234 If the plot showing the time delayed mutual information shows a marked minimum that value
235 can be considered as a responsible time delay; Fig 3 shows the mutual information plotted
236 against time delay. Likewise, the minimal embedding dimension, which correspond to the
237 minimum number of the false nearest neighbours can be treated as the optimum value of
238 embedding dimension in (Unnikrishnan et al.,2006, Unnikrishnan, 2010). A plot of fraction of
239 false nearest neighbours against embedding dimension can be seen in Fig 4. It was observed that
240 for all the daily detrended TEC time series the choice of $\tau \geq 30$ and $m \geq 4$ values of delay and
241 embedding dimension above these values are suitable for analysis of data for all stations. The
242 choice of $\tau = 30$ and $m = 5$ were mostly used to analyze the dynamical aspects for all the
243 stations. The reconstructed Phase space trajectory is shown in Fig 5

244 3.1.2 Lyapunov Exponents

245 The Lyapunov exponent has been a very important quantifier for the determination of chaos in a
246 dynamical system. This quantifier is also used for the determination of chaos in time series,
247 representing natural systems like the ionosphere and magnetosphere (Unnikrishnan 2008, 2010).
248 A positive Lyapunov exponent indicates divergence of trajectory in one dimension, or alternative
249 an expansion of volume, which can also be said to indicate repulsion, or attraction from a fixed
250 point. A positive Lyapunov exponent indicates that there is evidence of chaos in a dissipative
251 deterministic system, where the positive Lyapunov exponent indicates divergence of trajectory in
252 one direction or expansion of value and a negative value shows convergence at trajectory or
253 contraction of volume along another direction.

254 The largest Lyapunov exponent (λ_1) can be used to determine the rate of divergence as indicated
255 by (Wolf et al.,1985)

256 Where

$$257 \lambda_1 = \lim_{r \rightarrow \infty} \frac{1}{t} \ln \frac{\Delta x(t)}{x(0)} = \lim_{r \rightarrow \infty} \frac{1}{t} \sum_{i=1}^t \ln \left(\frac{\Delta x(t_i)}{\Delta x(t_{i-1})} \right) \quad (5)$$

258 The Lyapunov exponent was computed for the TEC values measured from Different stations.
 259 The evolution in state space was scanned with $\tau = 30$, $m = 5$, is shown in fig 6. The day to day
 260 variations of the Lyapunov exponent was computed for the entire year to so as to study the
 261 annual trend of variation. This was implemented using the method introduced by Rosenstein
 262 (1993), and Hegger et al., (1994), both algorithms use very similar methods. Lyapunov
 263 exponents were also computed for varying time delay at constant embedding dimension and also
 264 for varying embedding dimension, to check for the stability with changes in trajectory. These can
 265 be seen in fig. 6b and 6c. The day to day values of Lyapunov exponent plotted for the Enugu
 266 station and for Toro station are shown in fig 7a to 7b. The plots of the day to day values show the
 267 transient variation of the ionosphere and a wavelike yearly pattern.

268 3.1.3 Correlation Dimension

269 Another relevant method to study the underlying dynamics or internal dynamics of a system is to
 270 evaluate the dimension of the system. The correlation dimension gives a good approximation of
 271 this as suggested by Grassberger and Procaccia (1983a; b). The correlation dimension is
 272 preferred over the box counting dimension because it takes into account the density of points on
 273 the attractor (Strogatz 1994). The correlation dimension D is defined as

$$274 \quad D = \lim_{r \rightarrow 0} \frac{\ln C(r)}{\ln r} \quad (6)$$

275 The term $C(r)$ is the correlation sum for radius (r) where for a small radius (r) the correlation
 276 sum can be seen as $C(r) \sim r^d$ for $r \rightarrow 0$. The correlation sum is dependent of the embedding
 277 dimension (m) of the reconstructed phase space and it is also dependent of the length of the time
 278 series N as follows

$$279 \quad C(r) = \frac{2}{N(N-1)} \sum_{i=1}^N \sum_{j=i+1}^N \Theta(r - \|y_i - y_j\|) \quad (7)$$

280 Where Θ is the Heaviside step function, with $\Theta(H) = 0$ if $H \leq 0$ and $\Theta(H) = 1$ for $H > 0$.

281 The correlation dimension was computed using the Theiler algorithm approach, with Theiler
 282 window (w) at 180. The Theiler window was chosen to be approximately equal to the product of
 283 m and τ . A similar approach to the computation of correlation dimension was used by
 284 Unnikrishnan and Ravindran (2010) to determine the correlation dimension of detrended TEC

285 data for some stations in India which lies within the equatorial region, like Nigeria. Ogunsua et
286 al., (2014) also used similar methods for some detrended TEC from Nigerian stations.

287 The correlation dimension for data taken for the quietest day of October 2011 and the most
288 disturbed day of October 2011 from Birnin Kebbi GPS TEC measuring station were represented
289 by Fig 8a and Fig 8b respectively. The correlation dimension saturates at $m \geq 4$ for the quietest
290 day of the month and at $m \geq 5$ for the most disturbed day. In this illustration the most disturbed
291 day of this month fall within the storm period of October 2011. The classification of days into
292 quiet and disturbed days in the month of October 2011 enables us to compare the quiet and storm
293 periods together while comparing the quiet days with some relatively disturbed days.

294 **3.1.4 Computation of Tsallis Entropy and Principles of Nonextensive Tsallis Entropy**

295 Entropy measures are very important statistical techniques that can be used to describe the
296 dynamical nature of a system. The Tsallis entropy can be used to describe the dynamical
297 complexity of a system and to also understand the nonlinear dynamics like chaos which may
298 exist in a natural system. The use of entropy measure as a method to describe the state of a
299 physical system has been employed into information theory for decades. The computation of
300 entropy allows us to describe the state of disorderliness in a system, one can generalize this same
301 concept to characterize the amount of information stored in more general probability
302 distributions (Kantz & Shrieber 2003, Balasis et al.,2009). The concept of information theory is
303 basically concerned with these principles. The information theory gives us an important
304 approach to time series analysis. If our time series which is a stream of numbers, is given as a
305 source of information such that this numbers are distributed according to some probability
306 distribution, and transitions between numbers occur with well-defined probabilities. One can
307 deduce same average behaviour of the system at a different point and for the future. The term
308 entropy is used in both physics and information theory to describe the amount of uncertainty or
309 information inherent in an object or system (Kantz and schrieber 2003). The state of an open
310 system is usually associated with a degree of uncertainty that can be quantified by the
311 Boltzmann-Gibbs entropy, a very useful uncertainty measure in statistical mechanics. However
312 Boltzmann-Gibbs entropy cannot, describe non-equilibrium physical systems with large
313 variability and multifractal structure such as the solar wind (Burgala et al., 2007, Balasis et al.,

314 2008). One of the crucial properties of the Boltzmann-Gibbs entropy in the context of classical
315 thermodynamics is extensivity, namely proportionality with the number of elements of the
316 system. The Boltzmann-Gibbs entropy satisfies this prescription if the subsystems are
317 statistically (quasi-) independent, or typically if the correlations within the system are essentially
318 local. In such cases the system is called extensive. In general however, the situation is not of this
319 type and correlations may be far from negligible at all scales. In such cases, the Boltzmann-
320 Gibbs entropy is nonextensive (Balasis et. al., 2008, 2009). These generalizations above were
321 proposed by Tsallis (1988), who was inspired by the probabilistic description of multifractal
322 geometries. Tsallis (1988, 1998) introduced an entropy measure by presenting an entropic
323 expression characterized by an index q which leads to a nonextensive statistics,

$$324 \quad S_q = k \frac{1}{q-1} \left(1 - \sum_{i=1}^W p_i^q \right) \quad (8)$$

325 Where p_i are the probabilities associated with the microscopic configurations, W is their total
326 number, q is a real number, and k is Boltzmann's constant. The value q is a measure of the
327 nonextensivity of the system: $q \rightarrow 1$ corresponds to the standard extensive Boltzmann-Gibbs
328 statistics. This is the basis of the so called nonextensive statistical mechanics, which generalizes
329 the Boltzmann-Gibbs theory. The entropic index q characterizes the degree of nonadditivity
330 reflected in the following pseudoadditivity rule:

$$331 \quad \frac{S_q(A+B)}{k} = \left[\frac{S_q(A)}{k} \right] + \left[\frac{S_q(B)}{k} \right] + (1-q) \left[\frac{S_q(A)}{k} \right] \left[\frac{S_q(B)}{k} \right]. \quad (9)$$

332 The cases $q > 1$ and $q < 1$, correspond to subadditivity (or subextensivity) and superadditivity
333 (or superextensivity), respectively and $q = 1$ represents additivity (or extensivity). For
334 subsystems that have special theory probability correlations, extensivity is not a valid for
335 Boltzmann-Gibbs entropy in such cases, but may occur for S_q with a particular value of the index
336 q . Such systems are sometimes referred to as nonextensive (Boon and Tsallis, 2005, Balasis et al
337 2008, 2009). The parameter q itself is not a measure of the complexity of the system, but
338 measures the degree of nonextensivity of the system. It is the time variations of the Tsallis
339 entropy for a given $q(S_q)$ that quantify the dynamic changes of the complexity of the system.
340 Lower S_q values characterize the portions of the signal with lower complexity. In this

341 presentation we estimate S_q on the basis of the concept of symbolic dynamics and by using the
342 technique of lumping (Balasis et al. 2008, 2009).

343 A comparison of Tsallis entropy with Lyapunov exponents computed for the same set of data has
344 been carried out in this work, to see the efficacy of the combined usage of both parameters. This
345 is based on the established facts that variations in the values of Tsallis entropy can be linked with
346 that of Lyapunov exponents chaotic behavior in systems as seen in (Baranger et al., 2012;
347 Anastasiadis et al., 2005; Kalogeropoulos et al., 2012;2013). Coraddu et al., (2005) showed the
348 Tsallis entropy generalization for Lyapunov exponents. Further details can be found in Ogunsua
349 et al., (2014),

350 they were able to investigate the similarities in their response to the complex dynamics of the
351 ionosphere, and this informs the further use of the two quantities as indices to study the day to
352 day variation of ionospheric behaviour in this work.

353 The values of these entropy measures were also computed in order to study the dynamical
354 complexity of the system under observation (the ionosphere). The day to day values of Tsallis
355 entropy were computed for the entire year for different stations. The day to day values of Tsallis
356 entropy plotted for the Enugu station and for Toro station are shown in fig 9(a and b). The plots
357 of the day to day values show the transient variation of the ionosphere and a wavelike yearly
358 pattern.

359 **3.2 Non linearity Test using surrogate data**

360 The test for non-linearity using the method of surrogate data according to Kantz and Schreiber
361 (2003) has proven to be a good test for non-linearity in time series describing a system. It has
362 been accepted that the method of surrogate data test could be a successful tool for the
363 identification of nonlinear deterministic structure in an experimental data (Pavlos et al., 1999).
364 This method involves creating a test of significance of difference between linearly developed
365 surrogate and original nonlinear time series to be tested. The test is done by carrying out the
366 computation of the same quantity on both surrogates and the original time series and then
367 checking for the significance of difference between the results obtained from the surrogates with
368 the original data. Theiler et al (1992) suggested the creation of surrogate data by using Monte

369 Carlo techniques for accurate results. According to this method, typical characteristic of data
370 under study are compared with those of stochastic signals (surrogates), which have the same
371 auto-correlation function and the power spectrum of the original time series. It can be safely
372 concluded from the test of significance carried out on the surrogate and the original data that, a
373 stationary linear Gaussian Stochastic model cannot describe the process under study provided
374 that the behaviour of the original data and the surrogate data are significantly different.

375
376 In this work 10 surrogate data were generated from the original data set. The geometrical and
377 dynamical characteristics of the original data were then compared to that of the surrogates using
378 the statistical method of significance of difference which can be defined as

379
380
$$S = \frac{\alpha_{Surr} - \alpha_{Original}}{\sigma} \quad (13)$$

381
382 Where α_{Surr} is the mean value of the computed quantity for the surrogate data and $\alpha_{Original}$ is
383 the same quantity computed for the original TEC data, σ is the standard deviation of the same
384 quantity computed for the surrogate data. The significance of difference considered for the null
385 hypothesis to be rejected here is greater than 2, which enables us to be able to reject the null
386 hypothesis that the original TEC data describing the ionospheric system can be modeled using a
387 Gaussian linear stochastic model with confidence greater than 95%.

388 The surrogate data test for all stations used in this study show that the Lyapunov exponent of
389 the surrogate data for the selected days in October are shown in the Table below The results
390 show that the surrogate data test for Lyapunov exponent show a significance of difference
391 greater than 2 for all the selected days for all the stations. Similar results were obtained for
392 Mutual Information, Fraction of False Nearest Neighbours and Correlation Dimension. This
393 result gives us the confidence to reject the null hypothesis that the data used cannot be modeled
394 using a linear Gaussian stochastic model, which shows that the system is a nonlinear system with
395 some level of determinism. Fig. 10 shows the plots comparing the mutual information plotted
396 against time delay for the original detrended data blue with the mutual information for the
397 surrogate data for TEC data measured at Lagos for the quietest day of March 2011, while Fig. 11
398 is comparing fraction of false nearest neighbours for the same set of data. Tables 2a shows the

399 values of Lyapunov exponents for both original detrended and its surrogate data for TEC
400 measured in Lagos during the quietest days and Table 2b shows the values of Lyapunov
401 exponents for both original detrended and its surrogate data for TEC measured in Lagos during
402 the most disturbed days of October 2011. **The result obtained from the surrogate data test shows**
403 **that we cannot represent the original detrended data with a linear Gaussian stochastic model.**

404 **3.3 Trend filtering using the moving average approach for the daily Values**

405 The trend of a fluctuating time series can be made clearer to reveal the general pattern of that
406 time series, and to make the fluctuating pattern of the daily variation of the chaoticity and
407 dynamical complexity measures clearer in the work, the moving average method has been
408 employed. The method of moving average filtering has found its applications geophysics (e.g.
409 Bloomfield 1992; Bloomfield and Nychka 1992; Baillie and Chung 2002), and in other areas like
410 financial time series analysis, microeconomics, biological sciences and medical sciences. The
411 various fields mentioned require different trend filtering method depending on the structure of
412 the time series to be analyzed. Different filtering processes that can be used to reveal the trend
413 includes the moving average filters, exponential filters, band-pass filtering, median filtering etc.

414 Suppose we have a time series $z[t]$ such that $t = 1, 2, 3 \dots \dots n$, where 'n' could assume any
415 value. If $z[t]$ consists of a consistent varying trend component that appears over a longer period
416 of time t given as $u[t]$ and a more rapidly varying component $v[t]$. The goal of trend filtering in
417 any research is to estimate either of the two components (Kim et al., 2009). The purpose of trend
418 filtering in this work is to further reveal the general slow varying trend that appears to be obvious
419 in the daily variation of the values of the chaoticity and dynamical complexity of the ionosphere,
420 which might appear to be obviously varying with the yearly solar activity (a quantity with slow
421 varying trend). To make $u[t]$ which represents the general slow varying trend smoother and in
422 the process reduce $v[t]$ we apply the moving average filter.

423 If we assume $z[t]$ to be our time series representing the daily variation of the values of the
424 chaoticity and dynamical complexity of the ionosphere, then our smoothing with weighting
425 vector/filter w_j will create the new sequence u_j as

$$426 \quad u[t] = z[t] * w[n] = \frac{1}{2k+1} \sum_{i=-k}^k x[n - i]. \quad (14)$$

427 In this work the Savitzky-Golay method of smoothing proposed by Savitzky and Goley (1967),
 428 which is a generalized form of moving average was applied to the trend smoothing of the daily
 429 variation of the chaoticity and dynamical complexity of the ionosphere. In this case it performs a
 430 least square fit to a small set of $L(= 2k + 1)$ consecutive data to a polynomial and then takes
 431 midpoint of the polynomial curve as output. The smoothed time series in this work will now be
 432 given as

$$433 \quad u[t] = z[t] * \omega[n] = \frac{\sum_{i=-k}^k A_i * x[n-1]}{\sum_{i=-k}^k A_i} \quad (15)$$

434 where, $\omega[n] = \frac{A_n}{\sum_{i=-k}^k A_i}$, $-k \leq n \leq k$ such that A_i controls the order of polynomial. A similar
 435 method was described in Reddy et al., (2010).

436 The smoothed daily variation and the original data and the plot of the smoothed variation only,
 437 for the Lyapunov exponents of the detrended TEC measured at the Enugu and Toro are shown in
 438 fig 12(a and b). The smoothed day to day variation for Tsallis entropy for the detrended TEC
 439 measured at Enugu and Toro stations respectively are shown in fig 13(a and b).

440 **4.0 DISCUSSION**

441 The results presented in the work reveals the dynamical characteristics of the ionosphere. These
 442 characteristics are being discussed in this section, considering the time series treatment and phase
 443 space reconstruction; the study of chaos using chaotic quantifiers and the use and comparison of
 444 dynamical complexity measures in terms of their response to the variations on ionospheric
 445 dynamics. Also being discussed, is the implication of the nonlinearity test using the surrogate
 446 data and the comparison of the two quantifiers and their viability as indices for the continuous
 447 study and characterization of the ionosphere

448
 449 The time series analysis shows the appearance of some degree of nonlinearity in the internal
 450 dynamics of the ionosphere. The time series plot in Fig. 1 shows the rise in TEC to peak at the
 451 sunlit hours of the day, however it can be seen that the rising to the peak exhibited by the
 452 ionosphere, which is the dominant dynamics during the day, make it impossible to clearly see the
 453 internal dynamics of the system from the TEC time series plot. It can be seen that the TEC time
 454 series curve is not a smooth curve with tiny variations, which probably describes a part of the

455 internal dynamics. These visible tiny variations around the edges of the time series plot can be
456 regarded as rate of change of TEC which is a phenomenon that can describe the influence of
457 scintillations in the ionosphere these variations are however more obvious during the night time
458 between 1100th and 1440th minutes of the day (that is, between about 1800 and 2400 hours of
459 the day). It should be noted here that scintillations has been described as a night time phenomena
460 associated with spread-F, and it occurs around pre-midnight and post-midnight periods (Vyas
461 and Chandra 1994; Vyas and Dayanandan 2011; Mukherjee et al.,2012; Bhattacharyya and
462 Pandit 2014). The detrended data shows the internal dynamics of the system more clearly, with a
463 pattern similar to the values around night period mentioned earlier. The post-sunset values
464 (especially at night time) in Fig.1 show a pattern similar pattern with the detrended TEC plot in
465 Fig 2. It has been established that TEC does not decrease totally throughout the night as expected
466 normally through simple theory that TEC builds up during the day, but it shows some anomalous
467 enhancements and variations and this can occur under a wide range of geophysical conditions
468 (Balan and Rao, 1987; Balan et al., 1991;Unnikrishnan and Ravindran, 2010). The delay
469 representation of the phase space reconstruction shows a trajectory that is clustered around its
470 origin, for all the stations, which can be seen as an indication of the possible presence of chaos.
471 The degree of closeness of these trajectories however varies for different days from one station
472 to another, resulting from varying degrees of variations in stochasticity and determinism. The
473 varying degrees of variations in stochasticity and determinism can be attributed to the daily
474 variations and local time variations of photoionization, recombination, influx of solar wind and
475 other factors that may influence the daily variations of TEC (Unnikrishnan 2010).

476
477 The positive values of Lyapunov exponent indicate the presence of chaos (Wolf et al., 1985;
478 Rosenstein et al., 1993; Hegger et al., 1999; Kantz and Schreiber, 2003). The presence of chaos
479 was revealed by the positive Lyapunov exponent computed from all stations and this as a result
480 of the fact that the ionosphere is a system controlled by many parameters influencing its internal
481 dynamics. Because of its extreme sensitivity to solar activity, the ionosphere is a very sensitive
482 monitor of solar events. The ionospheric structure and peak densities in the ionosphere vary
483 greatly with time (sunspot cycle, seasonally and diurnally), with geographical location (polar,
484 auroral zones, mild-latitudes, and equatorial regions), and with certain solar-related ionospheric
485 disturbances. During and following a geomagnetic storm, the ionospheric changes around the

486 globe, as observed from ground site can appear chaotic (Fuller-Rowell et al., 1994; Cosolini and
487 Chang, 2001; Unnikrishnan and Ravindran, 2010). The recorded presence of chaos as indicated
488 by the positive values of Lyapunov exponent was found in all the computations, for all the TEC
489 values obtained for the selected days from all the measuring stations used in this work. This can
490 be expected as it agrees with results from previous works that show that there is a reasonable
491 presence of chaos in the ionosphere, even in the midst of the influence of stochastic drivers like
492 solar wind (Bhattacharyya, 1990; Wernik and Yeh, 1994; Kumar et al., 2004; Unnikrishnan et
493 al., 2006a,b; Unnikrishnan, 2010). However the values of Lyapunov exponents vary from day to
494 day due to variations in ionospheric processes for different days on the same latitude as seen in
495 Fig. 7(a and b) with Fig. 12(a and b) showing the day to day variation (upper panel) and the
496 smoothed curve of the day to day variation (lower panel) for the entire year. There are also
497 latitudinal variations due to spatial variations in the various ionospheric processes taking place
498 simultaneously. The ionosphere is said to have a complex structure due to these varying
499 ionospheric processes.

500 The higher values of Lyapunov exponent during months of low solar activity (the solstices) is an
501 evidence that that the rate of exponential growth in infinitesimal perturbations in the ionosphere
502 leading to chaotic dynamics might be of higher degree during most of the days of those months
503 compared to days of the months with high solar activities showing lower values of Lyapunov
504 exponents (Unnikrishnan 2010, Unnikrishnan and Ravindran, 2010).

505
506 The results of the correlation dimension values computed are within the range of 2.7 to 3.2 with
507 the lower values occurring mostly during the storm periods. The lower dimension during the
508 storm periods compared to the quiet days may be due to the effect of a stochastic drivers like
509 strong solar wind and solar flares, that occurs during geomagnetic storms on the internal
510 dynamics of the ionosphere, this could have been as a result of the fact that the internal dynamics
511 must have been suppressed by the external influence. The restructuring of the internal dynamics
512 of the ionosphere might be responsible for low dimension chaos during storm and also the lower
513 values of other measures like the Lyapunov exponents. The relatively disturbed day however
514 might have a higher dimension so long as it is not a storm period, and sometimes a relatively
515 disturbed day of the month might be a day with storm and in this case there is usually a lower
516 value of chaoticity and sometimes lower values of correlation dimension as well. The lower

517 value of chaoticity and dimension in ionosphere during storms indicates a phase transition from
518 higher values during the quiet periods to lower values during storm periods which may be due to
519 the modification of the ionosphere by the influx of high intensity solar wind during the storm
520 period (Unnikrishnan et al., 2006a, b; Unnikrishnan 2010; Unnikrishnan and Ravindran, 2010).

521

522 The surrogate data test shows significance of difference greater than 2 for all the computed
523 measures which enables rejection of the null hypothesis that the ionospheric system can be
524 represented with a linear model for all the data used from the stations. However it was
525 discovered that the lower significance of difference corresponds to the lower values of Lyapunov
526 exponents during storm and extremely disturbed periods (see tables 2a and 2b 3). This may be
527 due the rise in stochasticity during the storm period as a result of drop in values of computed
528 quantities like Lyapunov exponents. Our ability to reject the Null hypothesis for all stations
529 however shows the presence of determinism and confirms that the underlying dynamics of the
530 ionosphere is mostly non-linear. This further validates the presence of chaos since the surrogate
531 data test for non-linearity show that our detrended TEC is not a Gaussian (linear) stochastic
532 signal (Unnikrishnan 2010). However for some of the data sets the saturation of the average
533 mutual information observed at delay close to unity (as seen in fig. 3) and the saturation
534 Lyapunov exponent in the first time step (Fig. 6) indicate that there could be a high influence of
535 stochasticity in the system.

536

537

538 The Tsallis entropy was able to show the deterministic behavior of the ionosphere considering
539 its response during storm periods compared to other relatively quiet periods as the rapid drop in
540 values of Tsallis entropy during storm show that there is a transition from higher complexity
541 during quiet period to lower complexity during storms, this response in the values of Tsallis
542 entropy is similar to the response of Lyapunov exponent values during storm. This reaction to
543 storm shown by the values of Tsallis entropy computed for TEC was also described by the
544 reaction of Tsallis entropy computed for Dst during storm periods (Balasis et al., 2008, 2009). A
545 closer observation of the day-to-day variability within a month shows that the values were much
546 lower for storm periods compared to the nearest relative quiet period. For example, the storm
547 that occurred on the 25th of October resulted in lower values of Lyapunov exponent and Tsallis

548 entropy compared to relatively quiet days close to it. The reaction to storm may be due to the
549 influence of stochastic driver like strong solar wind flowing into the system as a result of solar
550 flare or CMEs that produces the geomagnetic storms. Although there is always an influence of
551 corpuscular radiation in form of solar wind flowing from the sun into the ionosphere, the
552 influence is usually low for days without storm compared to days with geomagnetic storms as a
553 result of solar flares, CMEs etc (Unnikrishnan et al., 2006a,b; Unnikrishnan, 2010, Ogunsua et al
554 2014).

555

556 The presence of chaos and high variations in the dynamical complexity, even at quiet periods in
557 the ionosphere may be due to the internal dynamics and inherent irregularities of the ionosphere
558 which exhibit non-linear properties. However, this inherent dynamics may be complicated by
559 external factors like Geomagnetic storms. This may be the main reason for the drop in the values
560 of Lyapunov exponent and Tsallis entropy during storms. According to Unnikrishnan et al.,
561 (2006a,b), geomagnetic storms are extreme forms of space weather, during which external
562 driving forces , mainly due to solar wind, subsequent plasmasphere -ionosphere coupling, and
563 related disturbed electric field and wind patterns will develop. This in turn creates many active
564 degrees of freedom with various levels of coupling among them, which alters and modifies the
565 quiet time states of ionosphere, during a storm period. This new situation developed by a storm,
566 may modify the stability/instability conditions of ionosphere, due to the superposition of various
567 active degrees of freedom.

568

569 The observation from the day-to-day variability of Lyapunov exponent and Tsallis entropy also
570 show irregular pattern for all stations. These irregular variations might be due to the same factors
571 mentioned before (i.e internal irregularities due to so many factors described and also due to
572 variation in the influx of the external stochastic drivers). The day-to-day variability for the entire
573 year shows a “wavelike” pattern with the values dropping to lower values during the equinox
574 months especially during March-April equinox. This can be seen as a form of semiannual
575 variation, possibly resulting from the higher energy inputs during equinoxes. This is because
576 solar wind is maximized at the equinoxes which might result in higher energy input that will
577 eventually suppress the internal dynamics to give lower values of chaoticity. The modification of
578 the ionosphere as a result of the higher energy input resulting from the maximized influx of solar

579 wind has been reported to be responsible for the lower values of chaoticity when averagely
580 compared to the days of the year with lower solar wind inputs as reported by Unnikrishnan et al.,
581 2006; 2010; Ogunsua et al., 2014. The semiannual pattern has been found to be similar for
582 different stations as seen in Figs. 7 & 12 and Figs. 9 & 13 for Lyapunov exponents and Tsallis
583 entropy respectively. Figs. 9 and 13 show the smoothed curves for Lyapunov exponent and
584 Tsallis entropy respectively, with the drop in values at equinoxes showing more clearly. The
585 phase transition in chaoticity and dynamical complexity is also responsible for the wavelike
586 variations, with values of Lyapunov exponent and Tsallis entropy dropping during the equinoxial
587 months, and this may be due to the influence of the daily influx of the solar wind having higher
588 values during equinoxes due to the proximity of the Earth to the sun during this period compared
589 to the solstice months.

590
591 The wavelike pattern observed has been described to be as a result of self organized critical
592 (SOC) phenomenon, a phenomenon which has been found to exist in both the magnetosphere
593 and the ionosphere or the space plasma system in general, due to coupling between the two
594 systems, since the magnetosphere couples the ionosphere tightly to the solar wind (Lui, 2002).
595 Many literatures has shown the existence of chaos in the SOC in the magnetosphere (chang et
596 al., 1992, 1998, 1999; Consolini et al., 1996 Chapman et al., 1998; Freeman and Watkins 2002
597 and; Koselov and Koselova, 2001. Uritsky et al., (2003) and; Chang et al., (1992). The existence
598 of SOC in space plasma system involving both the ionosphere the the magnetosphere was
599 described by (Lui, 2002; Chang et al., 2002; Chang et al., 2004)

600
601 The variation along the latitude also shows the inconsistency and complexity of the ionospheric
602 processes. This is the reason why for the same day of the month the values of Lyapunov
603 exponent vary from one station to another. Lyapunov exponent however, appears to respond
604 better to changes in solar activities compared to Tsallis entropy with more distinct results. This
605 may be due to the fact that Tsallis entropy being not only a measure of complexity, but also a
606 measure of disorderliness in a system might not be as perfect in describing chaos as Lyapunov
607 exponent. Kalogeropoulos (2009) and Baranger et al (2002) observed that Tsallis entropy has a
608 relationship that is not totally linear in all cases at different level of chaos with Lyapunov
609 exponent as a measure of chaos.

610
611 There are also many variations in the internal dynamics of the ionosphere that could lead to
612 changes in chaotic behavior. The variations of Lyapunov exponents during quiet days might be
613 as a result of different variations in the intrinsic dynamics of the ionosphere. Difference in
614 variation pattern at different stations for the same quiet day might also be due to the same reason.
615 It can be affirmed that the ionosphere is a complex system that varies with a short latitudinal or
616 longitudinal interval such that even stations with one or two degrees of latitudinal differences
617 might record different values on the same day for both quiet and disturbed periods and that the
618 same might also occur for storm periods. This is illustrated by the different pattern of variation of
619 TEC recorded from different stations within such a close range as used in this study.

620
621 These Latitudinal variation in the values of Lyapunov exponents and Tsallis entropy can be
622 further described by the behavior of the TEC because there can be a more sporadic rate of
623 change in TEC as seen in the time series plots as a result of irregularities in the internal dynamics
624 of the ionosphere, which might be as a result of plasma bubbles. Irregularities develop in the
625 evening hours at F region altitudes of magnetic equator, in the form of depletions, frequently
626 referred to as bubbles. The edges of these depletions are very sharp resulting in large time rate of
627 TEC in the equatorial ionosphere, even during magnetically quiet conditions. The large gradient
628 of the equatorial ionization persists in the local post-sunset hours till about 2100 h LT.
629 (DasGupta et al., 2007; Unnikrishnan and Ravindran, 2010). The TEC data for one station might
630 experience an extremely sharp rate of change in TEC that may be due to some plasma bubbles in
631 that region while the TEC from the other station stays normal. These variations in the various
632 internal dynamics like plasma bubbles leading to scintillation can cause variations in the
633 dynamical response of the TEC. Hence, the irregular variation in the values of the Lyapunov
634 exponent and Tsallis entropy even in quiet periods for two relatively close stations may be due to
635 these irregularities. This might also be responsible for the quiet days in the same station having
636 lower values of Lyapunov exponent compared to higher values recorded for disturbed days
637 without the external influence of storms.

638
639 The variations of these chaos and dynamical complexity parameters might also be as a result of
640 the anomalous TEC enhancements that might occur at nights (Balan and Rao (1987); Balan et

641 al., 1991). These effects can also be seen more clearly in the Tsallis entropy values for the five
642 period window for quiet day of January, 2011, because the night time value is higher and it also
643 show a much higher series of fluctuations during this period compared to other periods. As
644 mentioned in Unnikrishnan and Ravindran (2010), the irregular changes in the dynamical
645 characteristics of TEC from the results of Lyapunov exponent and Tsallis entropy also may be
646 due to the collisional Raleigh-Taylor instability which may give rise to a few large irregularities
647 in L band measurements (Rama Rao et al., 2006; Sripathi et al., 2008) all these can be seen as
648 internal factors responsible for variations in the dynamical response of TEC as recorded from the
649 values of the Lyapunov exponents and Tsallis entropy completed for days without storm which
650 might be quiet or disturbed according to classification and also could account for higher values
651 of these qualifiers during disturbed days compared quiet days. During storms however, the
652 values were much lower

653
654 Earlier we, (Ogunsua et al., 2014) showed the appearance and variation of chaoticity quiet and
655 disturbed day classification by international most quiet day (IQD) and internal most disturbed
656 day (IDD) classification, as compared to quiet and storm period used by Unnikrishnan (2006;
657 2010). We were able establish that a relatively quiet day may be less chaotic compared to a
658 relatively disturbed day unlike the result presented by Unnikrishnan (2006; 2010) for quiet and
659 storm period. Also the combined use of both Lyapunov exponent and Tsallis entropy for the first
660 time was found to have a high correlation mostly above 80%, which has stimulated the interest
661 for further research using the two diagnosis for the study of ionospheric dynamics.

662
663 This work on the other hand presents the results for day to day variation and has revealed a
664 seasonal trend for both Lyapunov exponents and Tsallis entropy, which appear in wavelike in
665 form, with troughs during the two equinoxes. This was established for different stations used in
666 this research work. The results show the appearance of seasonal trend in spite of the sporadic
667 daily variation resulting from various changes in the internal dynamics. The seasonal trend has
668 provided another possible evidence of higher energy input during equinoxes, since it reveals the
669 effect of the annual energy input to the ionosphere. The day to day response these parameters has
670 also revealed the variations in the underlying dynamics of the system.

671

672 As a similarity between the present work and Ogunsua et al. (2014) the relationship between
673 Lyapunov exponent and Tsallis entropy can also be seen from this work, as the two quantifiers
674 exhibit similarities in their response to the dynamical behavior of the ionosphere with phase
675 transition at the same periods of time for all stations. A further investigation of this relationship
676 shows that all the daily values of Tsallis entropy correlates positively with the values of
677 Lyapunov exponent at values between 0.78 and 0.83.

678
679 The ability of these quantifiers to clearly reveal the ionospheric dynamical response to solar
680 activities and changes in its internal dynamics due to other factors is a valid proof of the
681 authenticity of the use of these chaotic and dynamical measures, as indices for ionospheric
682 studies.

683 **5.0 Conclusion**

684 The chaotic behaviour and dynamical complexity of low latitude ionosphere over some parts of
685 Nigeria was investigated using TEC time series measured Simultaneously at five different
686 stations namely Birnin Kebbi (geographic coordinates $12^{\circ}32'N$, $4^{\circ}12'E$; dip latitude $0.62^{\circ}N$),
687 Torro (geographic coordinates $10^{\circ}03'N$, $9^{\circ}04'E$; dip latitude $-0.82^{\circ}N$), Enugu (geographic
688 coordinates $6^{\circ}26'N$, $7^{\circ}30'E$; dip latitude $-3.21^{\circ}N$), Lagos (geographic coordinates $6^{\circ}27'N$,
689 $3^{\circ}23'E$; dip latitude $-3.07^{\circ}N$) and Yola (geographic coordinates $9^{\circ}12'N$, $12^{\circ}30'E$; dip
690 latitude $-1.39^{\circ}N$) within the low latitude region. The detrended TEC time series data obtained
691 from the GPS data measurement were analysed using different chaoticity and dynamical
692 complexity parameters.

693 The evidence of the presence of chaos in all the time series data was obtained for all the data
694 used, as indicated by the positive Lyapunov exponent. The results of Tsallis entropy show the
695 variations in the dynamical complexity of the ionosphere, which may be due to geomagnetic
696 storms and other phenomena like changes in the internal irregularities of the ionosphere. The
697 response of the Tsallis entropy to various changes in the ionosphere also shows the deterministic
698 nature of the system. The results of the Tsallis entropy show a lot of similarities with that of the
699 Lyapunov exponents between 0.78 and 0.81, with both results showing a phase transition from
700 higher values in the solstices to lower values during the equinoxial months. The values of
701 Lyapunov exponent were found lower for the days of the months in which storm was recorded

702 relative to the nearest relatively quiet days which agree with previous works by other
703 investigators. A similar pattern of results was obtained for the computed values of Tsallis
704 entropy. The random variations in the values of chaoticity in the detrended TEC describing the
705 internal dynamics of the ionosphere as seen in the result obtained from both Lyapunov exponent
706 and Tsallis entropy depicts the ionosphere as a system with a continuously changing internal
707 dynamics, which shows that the ionosphere is not totally deterministic but also has some
708 elements of stochasticity influencing its dynamical behaviour.

709

710 The phase transition in the systems of the ionosphere resulting in the lower values of the
711 chaoticity and dynamical complexity quantifiers during the geomagnetic storms and the
712 equinoxial months is the evidence that the ionosphere can be greatly modified by stochastic
713 drivers like solar wind and other incoming particle systems. The drop in values during equinoxes
714 can be seen as form of semiannual variation, a phenomenon peculiar to the low latitude regions.

715

716 Although the knowledge of being able to characterize the ionospheric behaviour using the two
717 major quantifiers shows their ability to measure level of determinism when used together, the
718 relationship between these two quantifiers calls for more research, in the use of these qualifiers,
719 to enable proper description and characterization of the state of ionosphere. The response of both
720 Tsallis entropy and Lyapunov exponents to changes in the ionosphere shows that the two
721 quantifiers can be used as indices to describe the processes/dynamics of the ionosphere.

722

723 ~~Even though we cannot conclude totally until further investigations have been carried out on~~
724 ~~various properties of the ionosphere describing its dynamics. It can be safely established that this~~
725 ~~study has created roadmap for the use of the chaoticity and dynamical complexity measures as~~
726 ~~indices to describe the process/dynamics of the ionosphere.~~

727

728

729

730

731

732

733

734

735 **Acknowledgement**

736 The authors appreciate the editorial team and the referees for their contributions which have led
737 to the final shape of this paper. The GPS data used for this research were obtained from the public
738 archives of the Office of the Surveyor General of the Federation (OSGoF) of the Federal
739 Government of Nigeria, which is the mapping agency of Nigeria.

740

741

742

743

744

745

746

747

748

749

750

751

752

753

754

755

756

757 **References**

758 Abdu M.A.: Major Phenomena of the equatorial ionosphere thermosphere system under
759 disturbed conditions, *J.Atmos.Solten Physics.*,59(13), 1505 – 1519, 1997.

760 Anastasiadis, A.; Costa, L.; Gonzáles, C.; Honey, C.; Széliga, M. & Terhesiu, D. "Measures of
761 Structural Complexity in Networks", *Complex Systems Summer School 2005, Santa Fe. (2005).*

762 Bak, P., C. Tang, and K. Wiesenfeld, Self-Organized Criticality-an Explanation of 1/F Noise,
763 *Phys. Rev. Lett.*, 59(4), 381– 384, 1987.

764 Balan N., Rao,P.B.; Latitudinal variations of nighttime enhancements in total electron content,
765 *journal of Geophysical Research* 92 (A4), 3436 – 3440. 1987

766 Balan N., Bailey G.J., Balachandian. Nouv R.: Solar and Magnetic effects on the latitudinal
767 variations of nighttime TEC enhancement, *Annales Geophysicae* 9, 60 – 69. 1991

768 Balasis, G., and Manda M.: Can electromagnetic disturbances related to the recent great
769 earthquakes be detected by satellite magnetometers? *Tectonophysis* – 431, doi:
770 10.1016/j.tecto.2006.05.038. 2007

771 Balasis, G., Daglis I.A., Papadimitrou, C., Kalimeri, M., Anastasiadis, A., Eftaxias, K.:
772 Dynamical complexity in D_{st} time series using non-extensive Tsallis entropy. *Geophysical*
773 *Research Letters* 35, L14102, doi:10.1029/2008GL034743. 2008

774 Balasis, G., Daglis I.A., Papadimitrou, C., Kalimeri, M., Anastasiadis, A., Eftaxias, K.:
775 Investigating Dynamical complexity in the magnetosphere using various entropy measures.
776 *Journal of Geophysical Research* 114, A00D06, doi:10.1029/2008JA014035. 2009

777 Ballie R. Chung S.: Modeling and forecasting from trend stationary long memory models, with
778 applications in climatology. *International journal of forecasting*, 18(2)215-226,2002.

779 Bhattacharyya, A: Chaotic behavior of ionosphere turbulence from scintillation measurements, J.
780 Geophys. Res, 17, 733 – 738, 1990.

781 Bhattacharyya, A and Pandit J.: Seasonal variation of spread-F occurrence probability at low
782 latitude and its relation with sunspot number. *International Journal of Electronics and*
783 *Communication technology* vol 5(2) pp. 40-43. 2014.

784 Bloomfeld P.: Trends in global Temperature. *Climate Change*, 21:1-16,1992

785 Bloomfeld P. and Nychka D.: Climate spectra and detecting climate change. *Climate Change*,
786 21:275-287,1992

787 Boon J., and C.Tsallis (Eds.): Nonextensive statistical mechanics: New trends, new
788 perspectives, *Europhys.Newss*, 36(6), 185 – 231. 2005

789 Burgula,L.F., A.F –Vixas, and C.Wang , Tsallis distribution of magnetic field strength variations
790 in the heliosphere: 5 to 90 AU, *J. Geophys. Res*, 112, A07206, doi: 10.1029/2006
791 JA012213.2007

792 Chang, T., Low-Dimensional Behavior and Symmetry-Breaking of Stochastic-Systems Near
793 Criticality-Can These Effects Be Observed in Space and in the Laboratory, *IEEE Trans. On*
794 *Plasma Sci.*, 20(6), 691– 694, 1992.

795 Chang, T.: Sporadic localized reconnection and multiscale intermittent turbulence in the
796 magnetotail, *AGU Monograph No. 104, Geospace Mass and Energy Flow*, (Eds) Horwitz, J. L.,
797 Gallagher, D. L., and Peterson, W. K., p. 193, (American Geophysical Union, Washington, D.
798 C.), 1998

799 Chang, T., Self-organized criticality, multi-fractal spectra, sporadic localized reconnections and
800 intermittent turbulence in the magnetotail, *Phys. of Plasmas*, 6(11), 4137–4145, 1999.

801

802 Chapman, S. C., Watkins, N. W., Dendy, R. O., Helander, P., and Rowlands, G.: A simple
803 avalanche model as an analogue for magnetospheric activity, *Geophys. Res. Lett.*, 25, 2397–
804 2400, 1998.

805 Coco I., Consolini, G., Amata, E., Marcucci, M.F., Ambrosino.: Dynamical changes in polar cap
806 potential structure: an information theory approach. *Nonlinear processes in geophysics.*, 18, 697-
807 707, 2011.

808 Consolini, G., Marcucci, M. F., and Candidi, M.: Multifractal structure of auroral electrojet index
809 data, *Phys. Rev. Lett.*, 76 (21), 4082–4085, 1996.

810 Coraddu, M.; Lissia, M.; Tonelli, R. Statistical descriptions of nonlinear systems at the onset of
811 chaos arXiv:cond-mat/0511736v1 30 Nov 2005 2005

812 Cosolini, G., Chang, T.: Magnetic field topology and criticality in geotail dynamics relevance to
813 substorm phenomena. *Space Science Reviews* 95, 309-321, 2001.

814 DasGupta, A., Das, A.: Ionospheric total electron content (TEC) studies with GPS in the
815 equatorial region, India *Journal of Radio and Space Physics* 36,278-292.2007.

816 Fraser A.M. and Swinney H.L.: independent coordinates for strange attractors from mutual
817 information, *Phys.Rev,A*, 33, 1134 – 1141, 1986.

818 Freeman, M. P., and N. W. Watkins, The heavens in a pile of sand, *Science*, 298, 979– 980, (1
819 November), 2002.

820 Fuller- Rowell, T.J., Codrescu, M.V., Moffett, R.J. Quegan, S.: Response of the magnetosphere
821 and ionosphere to geomagnetic storms. *Journal of geophysical Research* 99, 3893-3914, 1994.

822 Hegger R., Kantz, H., Shreiber, T.: Practical implementation of nonlinear time series method. The
823 Tisean package, *Chaos*.9, 413 – 430. 1994

824 Kantz, H. and Shreiber, T.: *Nonlinear time series analysis*. Cambridge university press pp. 69-70,
825 2nd Ed. 2003.

826 Kazimirovsky, E.S. and Vergasova, G.V., *Mesospheric, Lower Thermospheric Dynamics and*
827 *External Forcing Effects: A Review*, *Indian J. Radio Space Phys.*, vol. 38, no. 1, pp. 7–36, 2009.

828 Kazimirovsky, E.S., Kokourov, V.D., and Vergasova, G.V., Dynamical Climatology of the
829 Upper Mesosphere, Lower Thermosphere and Ionosphere, *Surv. Geophys.*, vol. 27, pp. 211–255,
830 2006.

831 Kennel, M.B., Brown, R., and Abarbanel, H.D.I.: Determining minimum embedding dimension
832 using a geometrical construction, *phys.Rev.A.*, 45, 3403 – 3411, 1992.

833 Kim S, Koh, K., Boyd S., and Gorivesky D.: L_1 Trend filtering. *SIAM Review*, 51(2):339-360,
834 2009.

835 Klobuchar, J.: Design and characteristics of the GPS ionospheric time-delay algorithm for single
836 frequency users, in: Proceedings of PLANS'86 – Position Location and Navigation Symposium,
837 Las Vegas, Nevada, 280–286, 4–7 November 1986.

838 Kozelov, B. V. and Kozelova, T. V.: Sandpile model analogy of the magnetosphere-ionosphere
839 substorm activity, Proc. Interball Meeting, Warsaw, Poland, 2001.

840

841 Kumar, K.S., Kumar, C.V.A., George, B., Renuka, G., and Venugopal, C.: Analysis of the
842 fluctuations of the total electron content, measured at Goose Bay using tools of nonlinear
843 methods, *J. Geophys. Res.*, 10, A02308, doi: 10.1029/2002/A009768, 2004.

844 Lui, A.T.Y.: Evaluation on the analogy between the dynamic magnetosphere and a forced and/or
845 self-organised critical system. *Nonlin. Process in Geophys.* 9: 399-407, 2002.

846 Mukherjee, S., Shivalika, S., Purohit, P. K., and Gwal, A. K.: Study of GPS ionospheric
847 scintillations over equatorial anomaly station Bhopal. *International Journal of Advances in Earth*
848 *Science*. Vol 1 (2). Pp. 39-48, 2002.

849 Ogunsua B. O., Laoye J. A., Fuwape I. A., Rabiou A. B.: The comparative study of chaoticity and
850 dynamical complexity in the equatorial/ low latitude region of the ionosphere over Nigeria
851 during quiet and disturbed days. *Nonlin process in Geophys* vol. 21, 127-142, 2014.

852 Pavlos, G.P., Kyriakov, G.A., Rigas, A.G., Liatsis, P.I., Trochoulos, P.C., and Tsonis, A.A.:
853 Evidence for strange attractor structures in space plasma, *Ann. Geophys.*, 10, 309 – 315, 1992,
854 <http://www.ann-geophys.net/10/309/1992/>

855 Perreault, P. and Akasofu, S.-I.: A study of geomagnetic storms, *Geophys. J. R. Astron. Soc.*, 54,
856 547–573, 1978.

857 Rabiou, A. B., Mamukuyomi, A. I., Joshua, E. O.: Variability of equatorial ionosphere inferred
858 from geomagnetic field measurement, *Bull. Astro Soc. India*. 35, 607-615. India. 2007

859 Rama Rao, P.V.S., Gopi Krishna, S., Niranjana, K., and Prasad, D.S.V.V.D.: Temporal and
860 Spatial variations in TEC using simultaneous measurements from the India GPS network of
861 receivers during the low solar activity period of 2004/2005, *Ann. Geophys.*, 24; 3279 – 3292,
862 doi: 10.5194/angeo-24-3279-2006, 2006.

863 Reddy D. S., Reddy N. G., Radhadevi P. V., Saibaba J., and Varadan G.: Peakwise smoothing of
864 data models using wavelets. *World Academy of Science, Engineering and Technology*, Vol:4
865 2010 03-24.

866 Remya, R., Unnikrishnan, K.: Chaotic Behaviour of interplanetary magnetic field under various
867 geomagnetic conditions. *Journal of atmospheric and solar terrestrial Physics*, 72, 662-675, 2010.

868 Rosenstein, M.T., Collins, J.J., DeLuca, C.J.: A practical method for calculation Largest
869 Lyapunov Exponents from small Data sets. *Physica D*. 65, 117, 1993.

870 Saito, A., Fukao, S., Mayazaki, S.: High resolution mapping of TEC perturbations with the GSI
871 GPS network over Japan. *Geophysical research letters*, 25, 3079-3082, 1998.

872 Savitzky A., Golay MJE, Smoothing and differentiation by simplified least square procedures.
873 *Analytical Chemistry* 1964, 36:1627-1639.

874 Shan, H., Hansen, P., Goertz, C. K., and Smith, K. A.: Chaotic appearance of the ae index, *J.*
875 *Geophys Res.*, 18(2), 147–150, 1991.

876

877 Sindelarova T., Buresova and D., Chum J.: Observations of acoustic-gravity waves in the
878 ionosphere generated by severe tropospheric weather. *Studia Geophysica et Geodaetica*, Volume
879 53, Issue 3, pp 403-418 2009. DOI:10.1007/s11200-009-0028-4

880

881 Tsallis,C: Possible generalization of Boltzmann _Gibbs statistics J.Stat.phys.,52,487-497. 1988

882 Tsallis,C: Generalised entropy-based criterion for consistent testing. Phys.Rev.E., 58, 1442 –
883 1445. 1998

884 Tsallis, C: Nonextensive statistics: theoretical, experimental and computational evidences and
885 connections. *Braz. J. Phys.* [online]. vol.29, n.1, pp. 1-35. ISSN 0103-9733 1999.

886 Unnikrishnan K.,Saito,A., and Fukao,S.: Differences in magnetic storm and quiet ionospheric
887 deterministic chaotic behavior. GPS TEC Analyses,J. Geophys Res,111, A06304, doi:
888 10.1029/2005 JA011311, 2006a

889 Unnikrishnan, K., Saito, A., and Fukao, S.: Differences in day and night time ionosphere
890 determine chaotic behavior : GPS TEC Analyses, J. Geophys. Res, 111, A07310, doi:
891 10.1029/2005 JA011313, 2006b.

892 Unnikrishnan, K.: comparison of chaotic aspects of magnetosphere under various physical
893 conditions using AE index time series *Ann. Geophysicae.*, 26, 941-953, 2008.

894 Unnikrishnan, K. Ravindran, S.: A study on chaotic behavior of equatorial/ low latitude
895 ionosphere over indian subcontinent, using Gps –TEC time series, *J. Atmo. Sol,-Ter. Phy.*, 72,
896 1080 – 1089, 2010.

897 Unnikrishnan, K.: Comparative study of chaoticity of Equatorial/low latitude ionosphere over
898 Indian subcontinent during geomagnetically quiet and disturbed periods. *Non Linear Processes in*
899 *Geophys*, 26, 941-953, 2010.

900

901 Uritsky, V. M., Klimas A. J., and Vassiliadis D.: Evaluation of spreading critical exponents
902 from the spatiotemporal evolution of emission regions in the nighttime aurora, *Geophys. Res.*
903 *Lett.*, 30(15), 1813, doi:10.1029/2002GL016556, 2003.

904

905 Vassiliadis, D.V., Sharma, A.S, Eastman, T.E., and Papadopoulos,K.: Low –dimensionless chaos
906 in magnetospheric activity from AE time series, *Geophys, Res, let.*, 17, 1841 – 1844, 1990.

907 Vyas, R. M., and Dayanandan B.: Night time VHF ionospheric scintillation characteristics near
908 crest of Appleton anomaly stations, Udaipur ($26^{\circ}N$ $73^{\circ}E$). Indian Journal of Radio and Space
909 physics. Vol 40 (4) pp. 191-202, 2011.

910 Vyas, G. D., and Chandra, H.: VHF scintillations and spread-F in the anomaly crest region.
911 Indian Journal of Radio and Space physics. Vol 23 pp. 157-164, 1994.

912 Wernik, A.W. and Yeh,K.C: Chaotic behavior of ionospheric scintillation medelling and
913 observations, Radio Sci., 29, 135 – 139, 1994.

914 Wolf, A., Swift,J.B, Swinney, H.L, and Vastano,J.A. : Determining Lyapunov exponents from a
915 time series, Physica D, 16, 285 – 317, doi: 10.1016/0167 -2789 (85) – 90011-9, 1985.

916

917

918

919

920

921

922

923

924

925

926

927

928

929

930 Table 1: Coordinates of the GPS stations

Station Name	Geographic Coordinates		Dip latitude ($^{\circ}N$)
	Long ($^{\circ}E$)	Lat($^{\circ}N$)	
Birnin Kebbi	$4^{\circ} 12' E$	$12^{\circ} 32' N$	$0.62^{\circ} N$
Torro	$9^{\circ} 04' E$	$10^{\circ} 03' N$	$-0.82^{\circ} N$
Yola	$12^{\circ} 30' E$	$9^{\circ} 12' N$	$-1.39^{\circ} N$
Lagos	$3^{\circ} 23' E$	$6^{\circ} 27' N$	$-3.07^{\circ} N$
Enugu	$7^{\circ} 30' E$	$6^{\circ} 26' N$	$-3.21^{\circ} N$

938 Table 2a : Results of Surrogate data test for Lyapunov exponent for TEC data for the quietest
939 days of October 2011 at Birnin Kebbi station.

Original Data	Surrogate data
0.1165	0.3921 ± 0.0420
0.0931	0.2029 ± 0.0756
0.1041	0.3860 ± 0.0741
0.0498	0.2891 ± 0.0598
0.1420.	0.3621 ± 0.0504

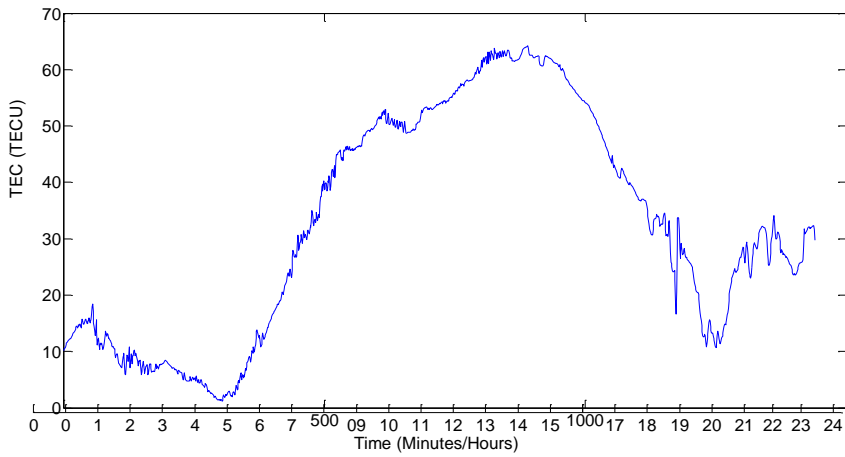
940

941 Table 2b: Results of Surrogate data test for Lyapunov exponent for TEC data for the most
942 disturbed days of October 2011 at Birnin Kebbi station.

Original Data	Surrogate data
0.0579	0.3039 ± 0.0541
0.0502	0.3156 ± 0.0428
0.0786	0.2527 ± 0.0296
0.1795	0.3662 ± 0.0468
0.1038	0.3100 ± 0.0416

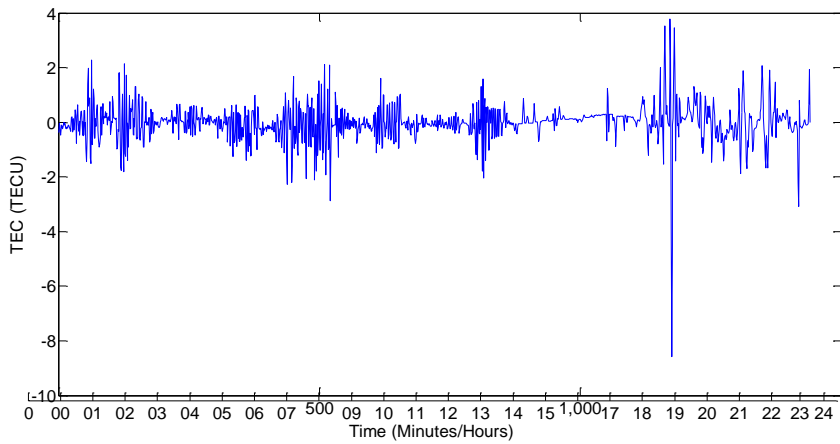
947

948



949

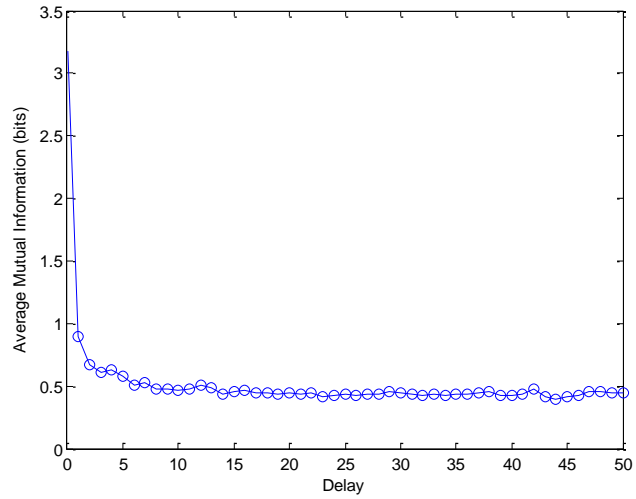
950 Fig 1. A typical time series plot for TEC measured at Lagos for 20 November 2011



951

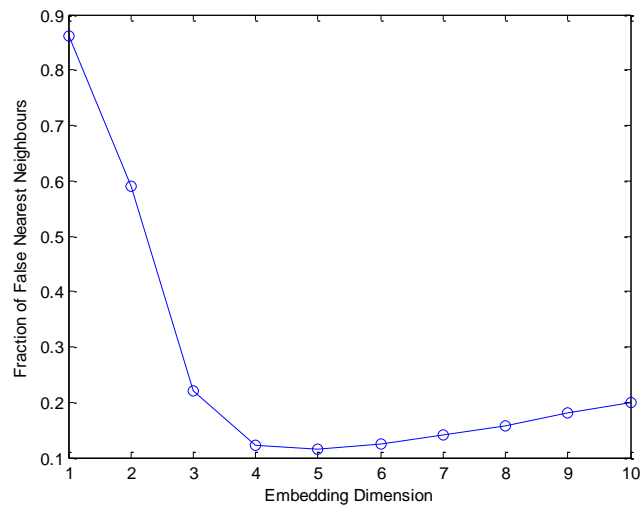
952 Fig 2. The detrended time series plot for TEC measured at Lagos

953



954

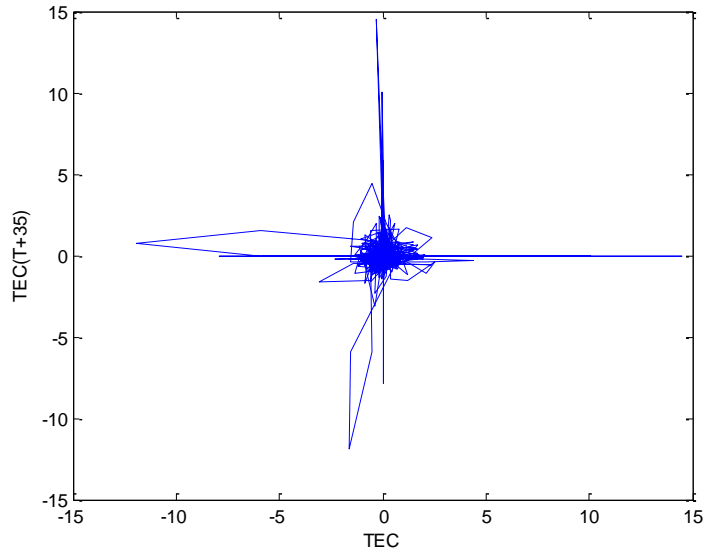
955 Fig. 3 Average mutual information against time Delay for TEC measured at Yola



956

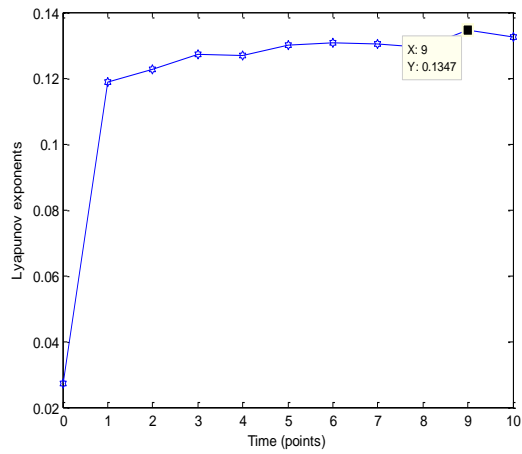
957 Fig. 4 Fraction of false nearest neighbours against embedding dimension for TEC measured at
 958 yola

959



960

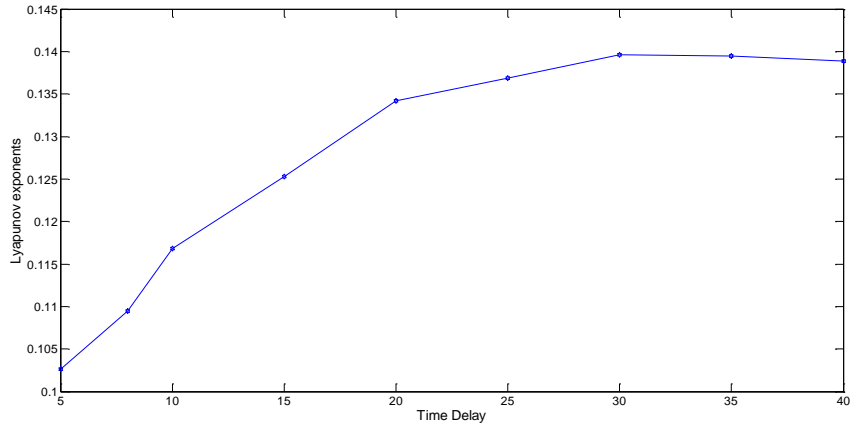
961 Fig.5 The Delay representation of the phase space reconstruction of the detrended TEC



962

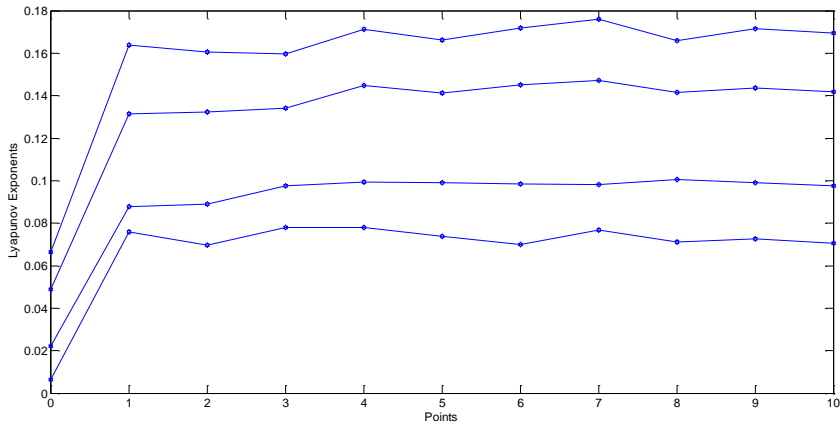
963 Fig. 6 Lyapunov Exponent computed and its evolution, computed as the state space trajectory
 964 scanned with $\tau=30$, $m=5$ for detrended time series measured at Yola with Largest Lyapunov
 965 Exponent equal to 0.1347.

966



967

968 Fig. 6b Lyapunov exponent computed for different time delay with a constant embedding
969 dimension.

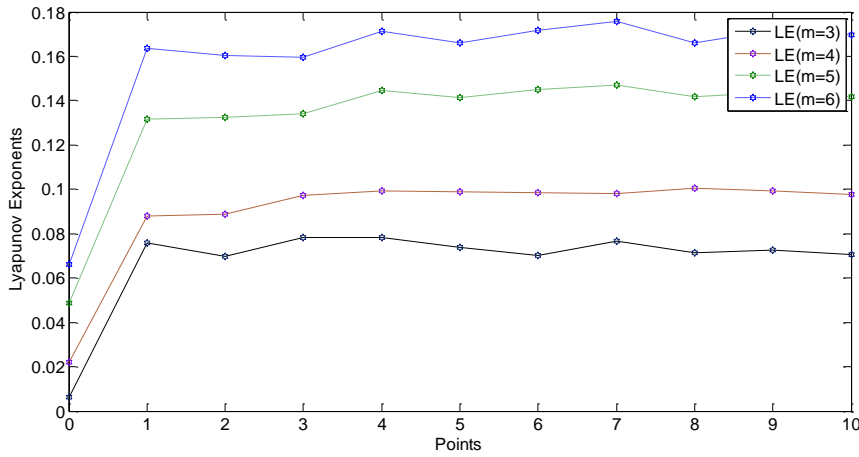


970

971 Fig. 6c Lyapunov exponents computed for different embedding dimension at constant time delay
972

973

974



Formatted: Font: (Default) Times New Roman, 12 pt

975

976

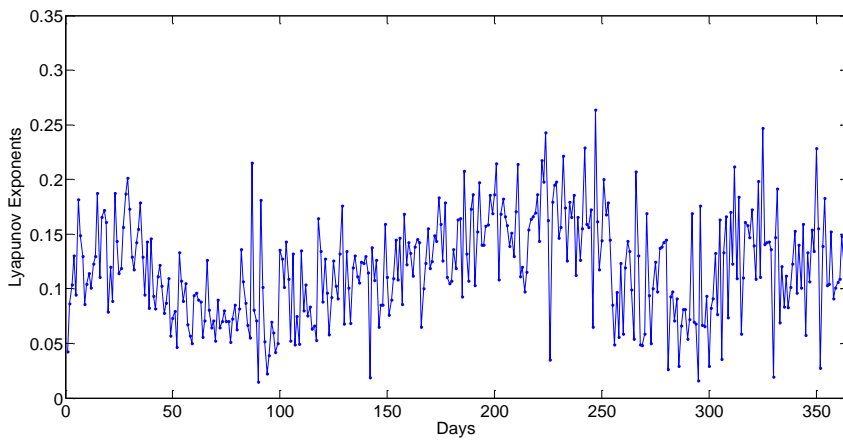
Fig. 6c Lyapunov exponents (LE) computed for different embedding dimension ($m= 3,4,5$ and 6) at constant time delay

977

978

979

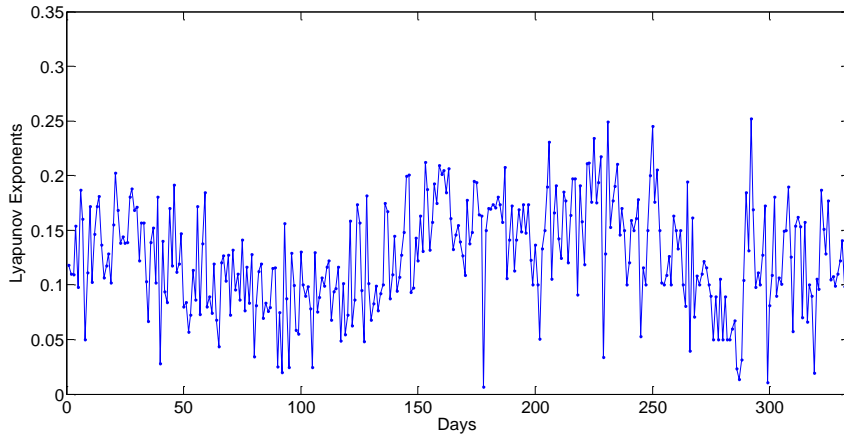
980



981

982 Fig. 7a The transient variations of Lyapunov exponents for 365 days of 2011 for detrended TEC
983 measured at Enugu

984

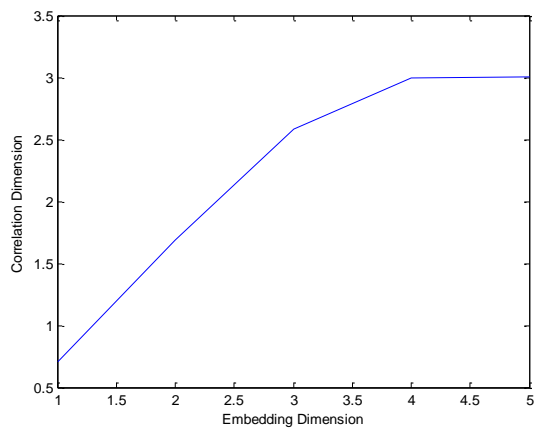


985

986 Fig. 7b The transient variations of Lyapunov exponents for 334 days (Jan1 –Nov30) of 2011 for
987 detrended TEC measured at Toro

988

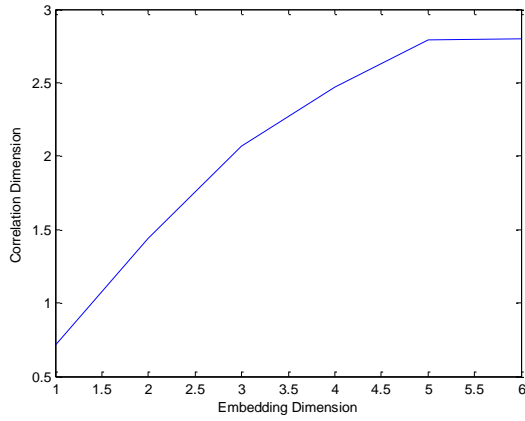
989



990

991 Fig. 8a The correlation dimension of the detrended TEC for the quietest day of October at Birnin
992 Kebbi which saturates at $m \geq 4$ and $\tau = 39$

993

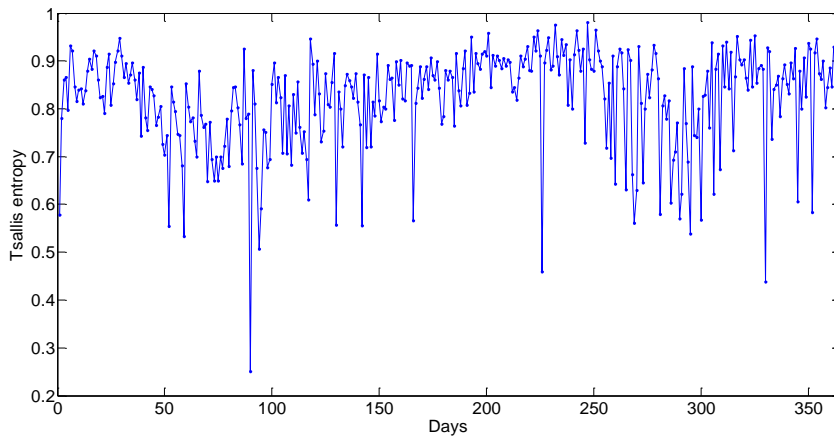


994

995

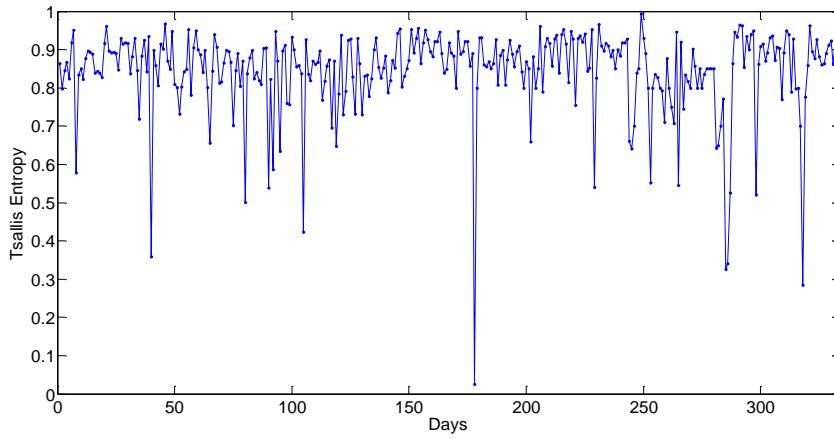
996 Fig. 8b The correlation dimension of the detrended for the most disturbed day of October at
997 Birnin Kebbi which saturates at $m \geq 5$ and $\tau = 34$

998



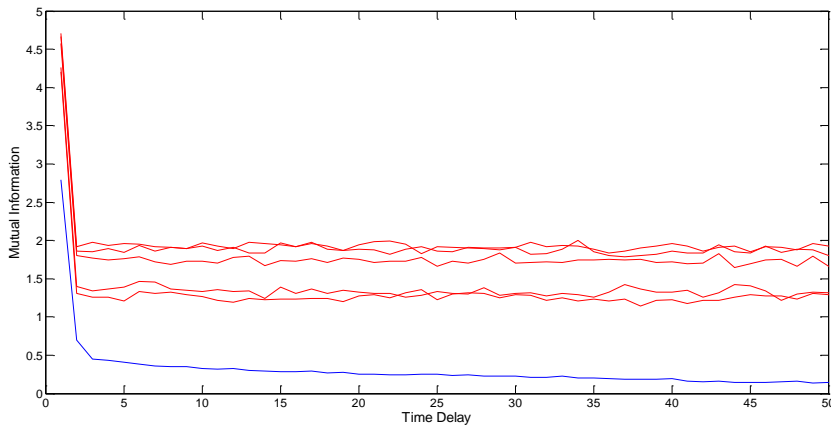
999

1000 Fig. 9a The transient variations of Tsallis Entropy for 365 days (Jan1 –Nov30) of 2011 for
1001 detrended TEC measured at Enugu



1002
1003 Fig. 9b The transient variations of Tsallis Entropy for 334 days (Jan1 –Nov30) of 2011 for
1004 detrended TEC measured at Toro

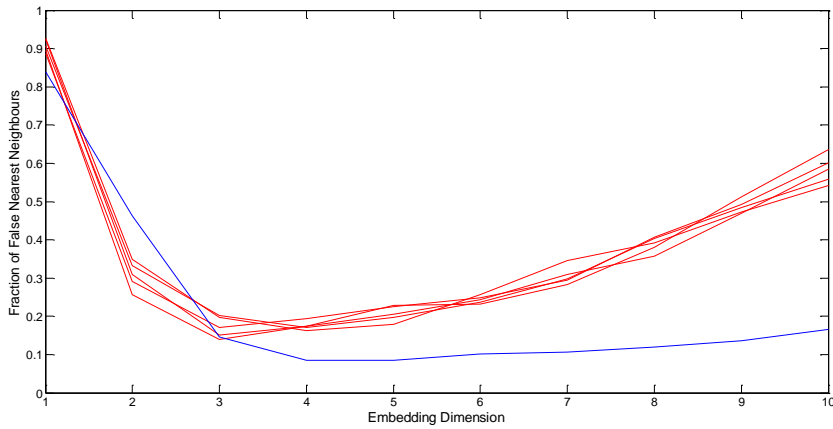
1005
1006



1007

1008 Fig 10 Mutual information plotted against time delay for the original detrended data in (blue
1009 curve) with the mutual information for the surrogate data (red curve) for TEC data measured at
1010 Lagos for the quietest day of march 2011

1011

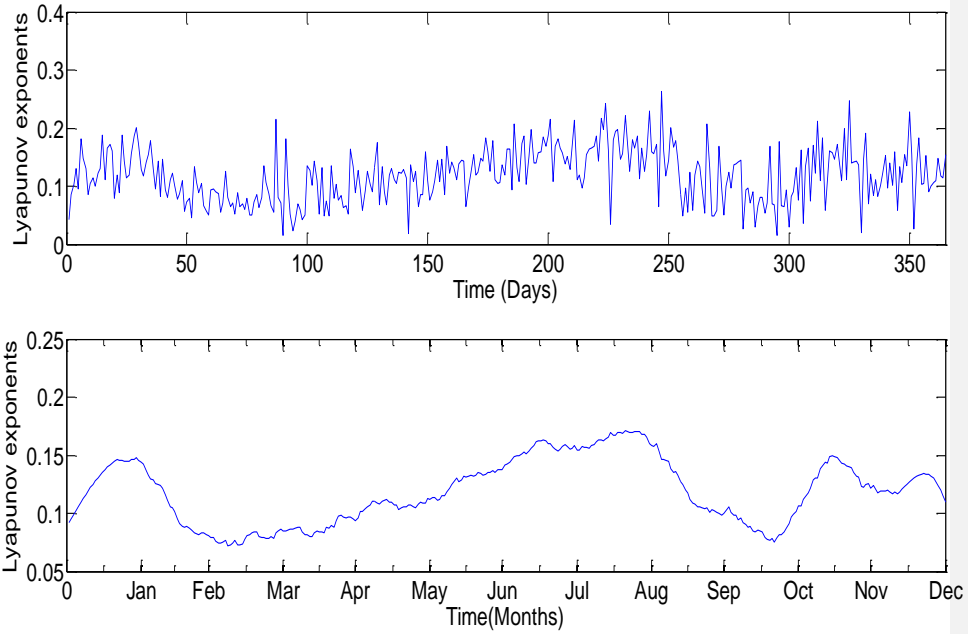


1012

1013 Fig 11 Fraction of false nearest neighbours plotted against time embedding dimension for the
1014 original detrended data in (blue curve) with the mutual information for the surrogate data (red
1015 curve) for TEC data measured at Lagos for the quietest day of march 20

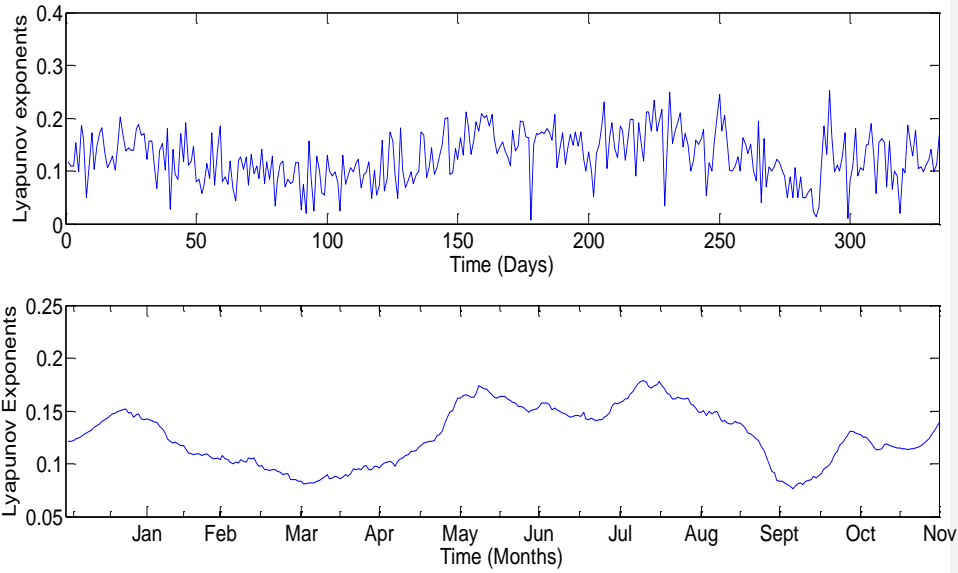
1016

1017



1018
 1019 Fig. 12a Daily variation of Lyapunov exponents for TEC measured at the Enugu station for the
 1020 year 2011 showing the Original data (Upper Panel) and the smoothed Plot of daily variation of
 1021 Lyapunov exponents for TEC measured at the Enugu station for the year 2011 (Lower panel)

1022
 1023
 1024
 1025
 1026
 1027
 1028



1029

1030

1031 Fig 12b Daily variation of Lyapunov exponents for TEC measured at the Toro station for the
 1032 year 2011 showing the Original data (Upper Panel) and the smoothed Plot of daily variation of
 1033 Lyapunov exponents for TEC measured at the Toro station for the year 2011 (Lower panel)

1034

1035

1036

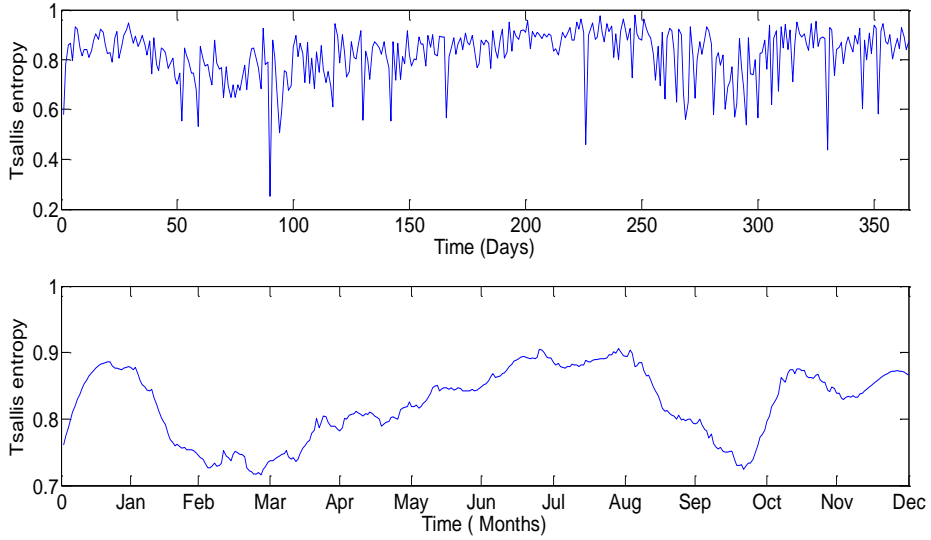
1037

1038

1039

1040

1041



1042

1043 Fig. 13a Daily variation of Tsallis entropy for TEC measured at the Enugu station for the year
 1044 2011 showing the Original data (Upper Panel) and the smoothed Plot of daily variation of
 1045 Lyapunov exponents for TEC measured at the Enugu station for the year 2011 (Lower panel)

1046

1047

1048

1049

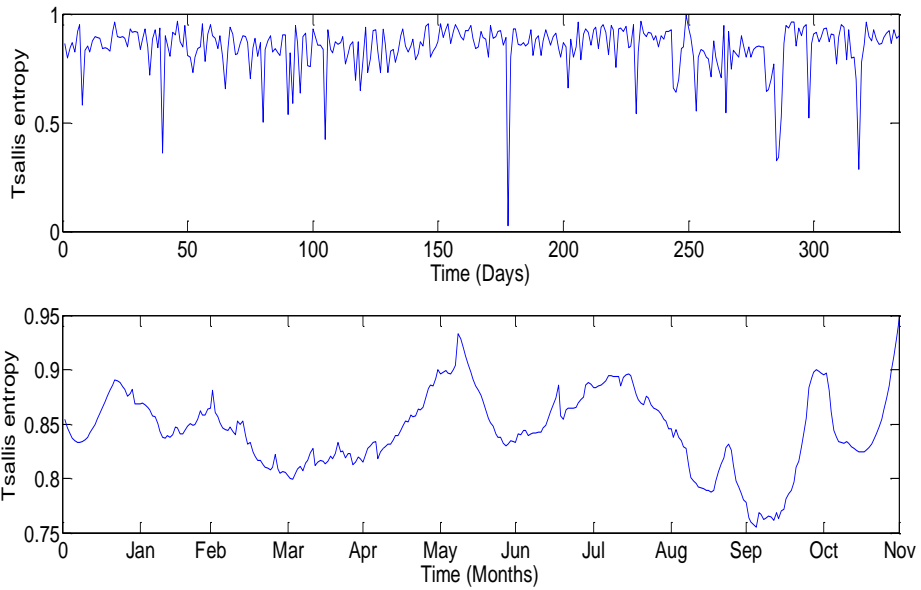
1050

1051

1052

1053

1054



1055

1056

1057 Fig. 13b Daily variation of Tsallis entropy for TEC measured at the Toro station for the year
 1058 2011 showing the Original data (Upper Panel) and the smoothed Plot of daily variation of
 1059 Lyapunov exponents for TEC measured at the Enugu station for the year 2011 (Lower panel)

1060

1061

1062

1063

1064

1065

1066

1067